NOMA Based Multiuser Uplink Signalling with Energy Harvesting IoT Nodes

Rajiv Kumar, Mayank Gupta, Kamal Agrawal, and Shankar Prakriya

***Abstract*—This paper investigates the performance of an uplink multiuser IoT network in which green self-sustaining IoT users utilize the energy harvested from the downlink signal for uplink signalling using NOMA principles. The uplink user with best link signal-to-noise (SNR) is first chosen. To increase spectral efficiency, another user is also picked for concurrent transmission using non-orthogonal multiple access (NOMA) principles. We demonstrate that the choice of the second user depends on the target rate and number of users, and is not always the user with the second-best SNR. The users are selected using a timer-based mechanism, and no feedback of channel estimates is involved. Considering the time-switching protocol for energy harvesting, we obtain expressions for outage probability and throughput of this scheme. Unlike in traditional uplink NOMA networks, the transmit powers here are random, and this makes the analysis and user selection mechanism interesting. Accuracy of the derived expressions is illustrated by computer simulations.**

***Index Terms*—Energy harvesting (EH), non-orthogonal multiple access (NOMA), time-switching (TS), outage probability, throughput.**

I. Introduction

The next generation of wireless communication networks is expected to facilitate high data rates and massive connectivity. The inclusion of the Internet of Things (IoT) and machine-type communication (MTC) has increased the demands for long-lasting battery life of communication nodes. To meet the requirements of massive connectivity, efficient spectrum utilization and high energy efficiency, the use of non-orthogonal multiple access (NOMA) and energy harvesting (EH) has been widely suggested in literature [1], [2].

The use of NOMA has been widely investigated for downlink networks where power domain multiplexing is used at the transmitter, and sophisticated multiuser detection using successive interference cancellation (SIC) is used at the receiver [3]. In contrast to downlink NOMA where power allocated to symbols of one user depends on power allocated to other users, in uplink NOMA each user transmits with its own power, and at the receiver, the user with the strongest channel gain is decoded first. Utilization of uplink NOMA opens up the possibilities for MTC where several low-power machine-type devices (MTDs) communicate to the access point (AP) [4]. Since IoT devices have limited battery energy, utilizing their own battery for information transmission can greatly limit their battery life and make frequent battery replacement necessary [5]. To avoid these battery replacements in sustainable IoT devices, the use of SWIPT-enabled green communication nodes has emerged as an appealing alternative [6]. The use of time-switching (TS) and power-splitting (PS) protocols for simultaneous wireless information and power transfer (SWIPT) has been extensively studied in literature [7]. EH-enabled uplink NOMA can help in providing better channel access to MTDs, thus improving the spectrum utilization efficiency as well as energy efficiency, which is the focus of this paper.

Compared to the downlink NOMA framework, literature on uplink NOMA enabled by self-sustaining communication nodes is relatively scarce. In [8], a wireless powered uplink NOMA network was studied where data rate and fairness were optimized for two decoding schemes, namely fixed and time sharing. In [9], the ergodic rate of SWIPT aided uplink hybrid NOMA network was analyzed. Further in [10], resource allocation schemes were studied to optimize the performance of the EH-assisted uplink NOMA network. In [11], a position-based user selection was investigated in the EH-aided uplink NOMA framework, where the effect of inter-cell interference was mitigated by carefully setting the base-station density. Further, in [12], a bidirectional relaying NOMA network was investigated, and expressions were derived for the ergodic capacity and outage probability.

In the EH-based uplink NOMA framework, enabling all users to transmit is not reasonable. This is because the amount of harvested energy is small and random. In such scenarios, user selection is essential for attaining higher SE as well as EE. In this work, we investigate a scenario in which multiple IoT users are present in the vicinity of the access point (AP). Out of the multiple users, the user having the best link signal-to-noise ratio (SNR) gets selected first - we refer to this as the orthogonal multiple access (OMA) scheme. In this work we allow one other user to transmit concurrently in a NOMA scheme. This work demonstrates that the best user to be selected for uplink transmission along with the user with the best SNR is not always the user with the second highest SNR - the choice depends on the target rate and the number of users. Further, based on the principles of order statistics, we analyze the performance of the considered system in terms of outage probability and the system throughput. Moreover, we show that with the proposed user selection, the system throughput can be maximized by a judicious choice of the TS parameter. The derived analytical expressions are validated through Monte Carlo simulations.

II. System Model

As illustrated in Fig. 1, we consider a communication network consisting of an access point (AP) and N IoT users $U_1, ..., U_N$. All IoT users are assumed to possess EH capability. Each IoT user utilizes the TS protocol for energy harvesting and information transmission. In TS, the signaling interval of

Rajiv Kumar, Mayank Gupta (Corresponding Author), Kamal Agrawal, and Shankar Prakriya are with the Department of Electrical Engineering, Indian Institute of Technology Delhi, New Delhi 110016, India (email: {eee202164, mayank.gupta, kamal.agrawal, shankar}@ee.iitd.ac.in). This work was supported by DST-SERB funding CRG/2021/000578.

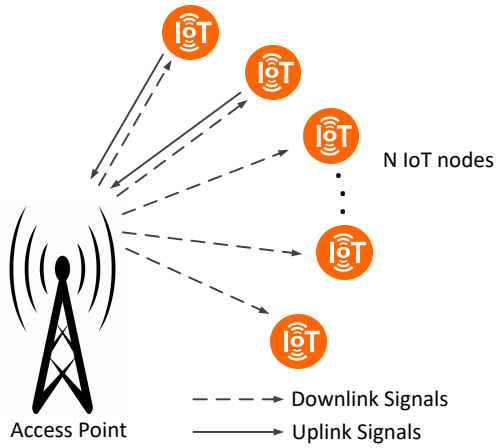

Fig. 1: EH powered uplink multiuser NOMA.

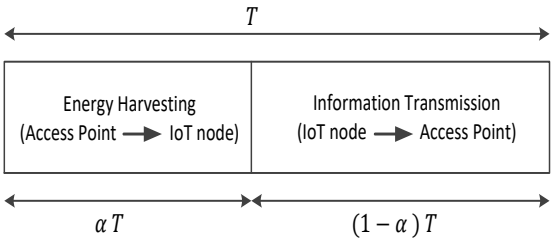

Fig. 2: Illustration of TS-EH protocol.

T duration is apportioned in the ratio $\alpha:(1-\alpha)$ as shown in Fig. 2 for EH and information transmission (IT), respectively, where $\alpha \in \{0,1\}$ is the TS coefficient. The IT occurs in two phases. In the first phase (of αT duration), IoT users harvest energy from the incoming AP's signal. In the second phase (of $(1-\alpha)T$ duration), information transmission takes place from the selected IoT users[1] to AP utilizing the harvested energy.

Independent and identically distributed (*i.i.d*) quasi-static Rayleigh faded reciprocal channels are assumed between AP and the IoT nodes. $h_k \sim \mathcal{CN}(0,\Omega)$ $(k \in (1,2\ldots,N))$ is the channel coefficient between the AP and the k^{th} IoT node. In the EH phase, y_k received at the IoT node U_k after matched filtering and sampling is

$$y_k = \sqrt{P}\ h_k\ s_e\ +\ n, \tag{1}$$

where $n \sim \mathcal{CN}(0,N_o)$ is the additive noise sample, s_e is the normalized symbol transmitted by AP (i.e $E(|s_e|^2)=1$), and P is the transmit power of the AP. The harvested energy Q_k at U_k during the EH phase in αT duration is given (neglecting energy from the noise) by

$$Q_k \quad = \quad \eta\ \alpha T\ P\ |h_k|^2, \tag{2}$$

where $\eta \in (0,1)$ denotes the energy harvesting efficiency of the EH circuit. Using Q_k, the transmitted power P_k of the IoT node U_k is given by

$$P_k \ = \ \frac{Q_k}{(1-\alpha)T} = \eta\frac{\alpha}{1-\alpha}P\ |h_k|^2. \tag{3}$$

If user U_k alone transmits in the next phase, the received signal z at the AP is $z = \sqrt{P_k}h_k s_k + n_a$, where $n_a \sim \mathcal{CN}(0,N_o)$. At the AP, the link SNR Γ_k of user U_k when it is signalling alone is

$$\Gamma_k \quad = \quad \eta\frac{\alpha}{1-\alpha}\frac{P}{\sigma^2}\ |h_k|^4. \tag{4}$$

Clearly, the channel coefficient $|h_k|^4$ is a Weibull-distributed random variable. Denote the order statistics of the link SNRs by $\Gamma_{(k)}$ so that

$$\Gamma_{(1)} \leq \ \ldots \leq\ \Gamma_{(m)}\ \leq\ \ldots\ \leq\ \Gamma_{(N)}. \tag{5}$$

Denote the corresponding users by $U_{(k)}$, the channels by $h_{(k)}$, and their symbols by $s_{(k)}$.

Let us consider that two users chosen for NOMA signalling are $U_{(n)}$ and $U_{(m)}$. We discuss the user selection scheme later in this paper. For the analysis, we assume that $U_{(n)}$ and user $U_{(m)}$ transmit unit-energy symbol $s_{(n)}$ and $s_{(m)}$ at information rates R. The sampled matched filter output z at AP in the second phase of signalling when both users transmit is given by

$$z = \sqrt{\frac{\eta\alpha P|h_{(n)}|^2}{1-\alpha}}h_{(n)}s_{(n)} + \sqrt{\frac{\eta\alpha P|h_{(m)}|^2}{1-\alpha}}h_{(m)}s_{(m)} + n_a. \tag{6}$$

The AP first decodes the symbols of user $U_{(n)}$. The (signal-to-interference-and-noise ratio (SINR) to decode the symbols of user $U_{(n)}$ can be expressed as

$$\Gamma_1 \quad = \quad \frac{\eta\frac{\alpha}{1-\alpha}P|h_{(n)}|^4}{\eta\frac{\alpha}{1-\alpha}P|h_{(m)}|^4 + N_o}. \tag{7}$$

After SIC, the SNR $\Gamma_{(m)}$ to decode symbols of user $U_{(m)}$ is

$$\Gamma_2 \quad = \quad \eta\frac{\alpha}{1-\alpha}\frac{P}{\sigma^2}|h_{(m)}|^4. \tag{8}$$

Before proceeding further, we discuss user selection scheme that will be used in the analysis. with $\gamma_{th} = 2^R - 1$, the outage probability P_o is written as

$$P_o \quad = \quad \Pr\{\Gamma_1 \geq \gamma_{th}, \Gamma_2 \geq \gamma_{th}\} \tag{9}$$

and the throughput τ then becomes

$$\tau \ = \ (1-\alpha)(1-P_o)\ 2R, \tag{10}$$

In the above expression, the term $1-\alpha$ appears due to the signalling duration used for IT. A factor of 2 appears since two users transmit concurrently.

A. User Selection

Intuitively it makes sense in accordance with the principles of NOMA to choose the user with the highest SNR such that $n = N$, so that the first user is $U_{(N)}$. This choice increases Γ_1 so that it can withstand interference from $U_{(m)}$, i.e., $\eta\frac{\alpha}{1-\alpha}P|h_{(m)}|^4$. Then, we look for the m that yields the highest throughput. However, throughput is still a function of α in addition to m, and the problem of selecting m^{th} user can be expressed as follows:

$$m \quad = \quad \arg\ \max_{\ell,\alpha}\ \tau(N,\ell,\alpha),$$

where we have written τ as a function of N, ℓ and α to emphasize its dependence on these choices. However, due to the complexity of the expression for throughput, evaluating an expression for m (throughput-optimal user selection) is not feasible. Numerical methods can readily be used to find the best value of m offline.

A timer-based mechanism is used to select the users. The AP transmits a pilot that the nodes use to determine the channel gain and set a timer inversely proportional to the channel gain. The timer of the node with the best link SNR goes to zero

[1]In this work, IoT users pair is selected where the first user is selected based on best SNR while the second best user is selected to ensure best throughput performance. A detailed explanation of the user selection scheme is provided later in this paper.

first, and it flags the AP - this is the user $U_{(N)}$. The AP waits for flags until the user $U_{(m)}$ is selected. All other IoTs reset their timers, and the first phase transmission of EH begins [13], [14]. To determine the m^{th} user, the steps are given in Algorithm 1.

Algorithm 1 Throughput-Optimal User Selection

1: Initialize $D = \{1,2,\ldots,N\}$, R, $\alpha \in (0,1)$
2: Evaluate $\gamma_{th} = 2^R - 1$
3: Select $U_{(N)}$ as the first user for NOMA Signalling. Since Γ_1 should be large enough to handle interference of other users.
4: Select $U_{(m)}$ user to accommodate with $U_{(N)}$ which gives best throughput such that

$$m \quad = \quad \arg \max_{\ell,\alpha} \tau(N,\ell,\alpha).$$

B. Order statistics of the Uplink link SNRs

Let $X_k = |h_k|^4$ where $k \in (1,2\ldots,N)$. Clearly, these are *i.i.d* random variables. The probability density function (PDF) $f_{X_k}(x_k)$ of random variable X_k is given by

$$f_{X_k}(x_k) = \frac{1}{4\ \Omega\ \sqrt{x_k}}\ \exp\left(-\frac{1}{2\ \Omega}\sqrt{x_k}\ \right) \tag{11}$$

The cumulative distribution function (CDF) of X_k is

$$F_{X_k}(x_k) = 1 -\ \exp\left(-\frac{1}{2\Omega}\sqrt{x_k}\ \right) \tag{12}$$

Denote the order statistics of X_k by $X_{(k)}$ so that

$$X_{(1)} < X_{(2)} < \ldots < X_{(N)} \tag{13}$$

The joint PDF of $X_{(N)}$ and $X_{(m)}$ [15] is as follows

$$f_{X_{(N)}\ ,X_{(m)}}(x_{(N)},x_{(m)}) = \frac{N!}{(N-m)!(m-2)!}(F_X(x_{(m)})^{N-m})$$
$$(F_X(x_{(N)}) - F_X(x_{(m)}))^{m-2} f_X(x_{(N)})\ f_X(x_{(m)}), \tag{14}$$

where $x_{(N)} > x_{(m)}$. In the analysis, we use these order statistics to derive outage probability and throughput expressions.

III. OUTAGE PROBABILITY ANALYSIS

For the notational convenience let us assume $|h_{(N)}|^4 = X_{(N)}$ and $|h_{(m)}|^4 = X_{(m)}$. So, we can rewrite (7) and (8) as

$$\Gamma_1 \quad = \quad \frac{\eta\frac{\alpha}{1-\alpha}PX_{(N)}}{\eta\frac{\alpha}{1-\alpha}PX_{(m)} + N_o}, \tag{15}$$

$$\Gamma_2 \quad = \quad \eta\frac{\alpha}{1-\alpha}\frac{P}{N_o}X_{(m)}. \tag{16}$$

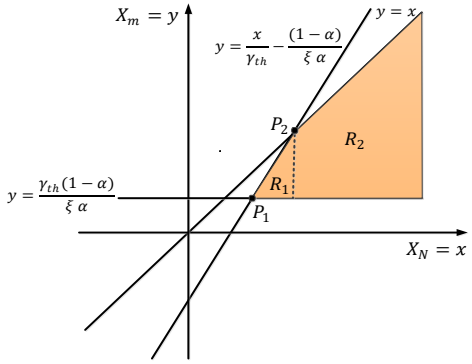

Fig. 3: Region to evaluate I_1 for $R \leq\ 1$.

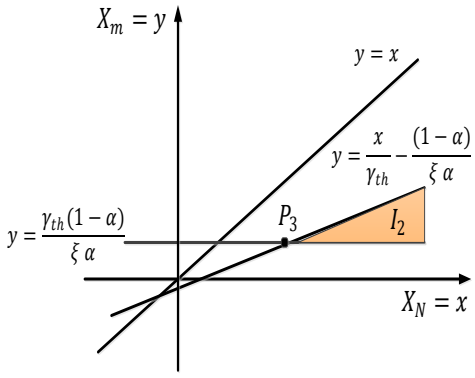

Fig. 4: Region to evaluate I_2 for $R > 1$.

We have

$$P_o = \Pr\ \{\ \Gamma_1\ \geq\ \gamma_{th}\ ,\ \Gamma_2\ \geq\ \gamma_{th}\ \}. \tag{17}$$

Using (15) and (16), we have

$$P_o \quad = \quad \Pr\left\{\frac{N_o\gamma_{th}(1-\alpha)}{\eta\alpha P} \ \leq\ X_{(m)}\ \leq\ \frac{X_{(N)}}{\gamma_{th}} - \frac{N_o(1-\alpha)}{\eta\alpha P}\right\}.$$

It is important to appreciate that as discussed in (14), $X_{(N)}$ and $X_{(m)}$ are dependent random variables. We evaluate I_1 using a graphical approach. It will be convenient to consider the case when $R \leq 1$ and $R \geq 1$ separately. The signalling outage can equivalently be written as

$$P_o \quad = \quad \begin{cases} 1 - \underbrace{\Pr\{\Gamma_1 \geq \gamma_{th}, \Gamma_2 \geq \gamma_{th}\}}_{I_1} & R \leq 1 \\ 1 - \underbrace{\Pr\{\Gamma_1 \geq \gamma_{th}, \Gamma_2 \geq \gamma_{th}\}}_{I_2} & R > 1 \end{cases} \tag{18}$$

Case 1: When $R \leq\ 1$.

Let $X_{(N)} = x$, $X_{(m)} = y$, and $\xi = \eta P/N_o$. In Fig. 3 we plot $X_{(N)}$ along the x-axis and $X_{(m)} =$ on the y-axis. R_1 and R_2 can be identified as the non-outage regions in the Fig. 3. The coordinate of points P_1 and P_2 are $\left(\frac{\gamma_{th}(1+\gamma_{th})(1-\alpha)}{\xi\alpha}, \frac{\gamma_{th}(1-\alpha)}{\xi\alpha}\right)$ and $\left(\frac{\gamma_{th}(1-\alpha)}{\xi\alpha(1-\gamma_{th})}, \frac{\gamma_{th}(1-\alpha)}{\xi\alpha(1-\gamma_{th})}\right)$ respectively in Fig. 3. We integrate the joint PDF in this region as

$$I_1 = \underbrace{\int_{x=\gamma_{th}(1+\gamma_{th})(1-\alpha)/\xi\alpha}^{\gamma_{th}(1-\alpha)/\xi\alpha(1-\gamma_{th})} \int_{y=\gamma_{th}(1-\alpha)/\xi\alpha}^{x/\gamma_{th}-(1-\alpha)/\xi\alpha} f_{XY}(x,y)\ dydx}_{R_1}$$
$$+ \underbrace{\int_{x=\gamma_{th}(1-\alpha)/\xi\alpha(1-\gamma_{th})}^{\infty} \int_{y=\gamma_{th}(1-\alpha)/\xi\alpha}^{x} f_{XY}(x,y)\ dydx}_{R_2} \tag{19}$$

Clearly

$$I_1 = R_1 + R_2. \tag{20}$$

Substituting for R_1 and R_2, simplifying using [16, eq. (1.111)] and integrating using change of variables, we have (21) and (22) shown at the top of the next page. The detailed proof is omitted due to the paucity of space. In (21), the integral does not have a closed form. However, it can readily be evaluated numerically. I_1 can be calculated from (20), (21) and (22) for $R \leq\ 1$.

Case 2: When $R > 1$

When the target rate is greater than unity, the non-outage region is shown in Fig. 4. The coordinate of point P_3 is $\left(\frac{\gamma_{th}(1+\gamma_{th})(1-\alpha)}{\xi\alpha}, \frac{\gamma_{th}(1-\alpha)}{\xi\alpha}\right)$ in Fig. 4. The non-outage $\overline{P}_o$ is

determined by evaluating the area under the curve when the $R > 1$ as

$$\overline{P}_o = I_2 = \int_{x=\gamma_{th}(1+\gamma_{th})(1-\alpha)/\xi\alpha}^{\infty} \int_{y=\gamma_{th}(1-\alpha)/\xi\alpha}^{x/\gamma_{th}-(1-\alpha)/\xi\alpha} f_{XY}(x,y)dydx \quad (24)$$

Using (14), for I_2, simplifying using [16, eq. (1.111)] and integrating using change of variables, we have (23) shown at the next page. In (23), the integral does not have a closed form. It can, however, be computed numerically. The outage probability is given as

$$P_o = \begin{cases} 1-I_1, & \text{when} \quad R \leq 1 \\ 1-I_2, & \text{when} \quad R > 1 \end{cases} \quad (25)$$

IV. THROUGHPUT MAXIMIZATION

Clearly, the throughput depends on the choice of α. This is because for $\alpha = 1$, the IoT users harvest the energy for the entire signalling duration and no information can be transmitted, and throughput remains zero. On the other hand, for $\alpha = 0$, no energy is available for information transmission, which also results in zero throughput. Therefore an optimal choice of TS parameter α is crucial to maximizing the throughput. for a fixed target rate R, the optimization problem can be formulated as

$$\alpha^* = \arg \max_{\alpha} \tau, \quad \text{s. t.} \quad 0 < \alpha < 1, \quad (26)$$

where α^* denotes the optimum TS parameter at which the throughput is maximized. Due to the involvement of complex mathematical functions in the expression for the outage probability in (25), it is impossible to obtain an accurate closed-form expression of the α^*. However, α^* can be determined using a one-dimensional offline search.

V. SIMULATION RESULTS

This section validates the derived analytical expressions through numerical simulations and provides useful insights regarding user selection and the TS EH parameter for various system parameters. We note that $\mathbb{E}\left[|h_i|^2\right] \propto d_i^{-\phi}$ where d_i is the distance between AP and IoT node U_k, ϕ (assumed to be 4) is the path-loss exponent and N (assumed to be 5) is the number of IoT users present in the vicinity of the AP. We assume $d_i = 1$ unit, and noise variance, $N_o = 1$. Unless mentioned otherwise, the other system parameters are considered as $P = 20$ dB, $\eta = 0.8$, $R = 2$ bpcu, and $\alpha = 0.2$.

Fig. 5 illustrates the variation of outage probability versus transmit power for different values of α. As anticipated, the outage probability decreases with increasing P (dB). We plot P_o for two different values of α, i.e., 0.1 and 0.4, and $R = 1$ bpcu. We observe that varying α significantly affects the P_o. The reasons for this have been discussed earlier. Analytical and simulation results match, confirming the correctness of the expressions.

Fig. 6 demonstrates the variation of throughput with transmit power P when the highest SNR user from the cluster is paired with $U_{(m)}$ for different values of m (user selection) for uplink transmission. Clearly, the derived expressions are validated by simulations. It is readily noticed that with increase in P, the throughput increases initially and gets saturated at higher values of transit power. This saturation is due to a fixed target rate and TS parameter. It is clear that m has to be chosen carefully, and the user with the second highest SNR is not the best choice. This is an important observation. It can be seen that this choice of m depends on P (it also depends on γ_{th}).

Fig. 7 demonstrates the variation of the throughput with α for different values of m (user selection mechanism). It can be noticed that the optimal value of the TS parameter is different for different user pairings. The choice of m depends on α. We observe that the throughput is a quasi-concave function of α. At $\alpha = 0$, no energy can be harvested by IoT users, which results in zero throughput. As α increases, the throughput also increases (more energy is available for information transmission). The throughput attains a maximum value at the optimum TS parameter. A further increase in α beyond α^* causes a reduction in the throughput as the information transmission time $(1-\alpha)T$ decreases. Therefore, a judicious choice of α is essential for maximizing the throughput. Further, it can also be observed that the best user to be selected for uplink transmission along with the user with the best SNR is not always the user with the second highest SNR - the choice depends on the target rate and the number of users.

Fig. 8 demonstrates the variation of the throughput with α for various R values. It is clearly noticed that, as expected, NOMA outperforms OMA at low target rates, and OMA is a

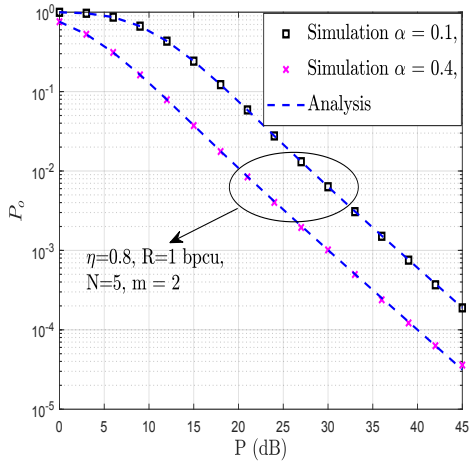

Fig. 5: P_o *vs* P (dB).

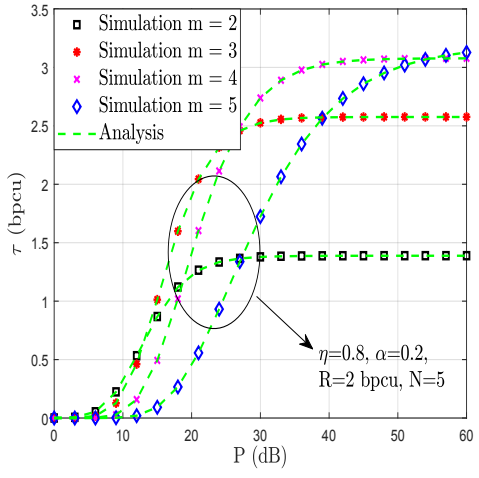

Fig. 6: τ *vs* P (dB).

$$R_1 = \sum_{k=0}^{m-2}\binom{m-2}{k}\frac{N!(-1)^{m-2-k}}{(N-m)!(m-2)!}\sum_{i=0}^{k}\binom{k}{i}\frac{(-1)^{k-i}}{k-i+N-m+1}\Bigg[\int_{x=\gamma_{th}(1+\gamma_{th})(1-\alpha)/\xi\alpha}^{\gamma_{th}(1-\alpha)/\xi\alpha(1-\gamma_{th})}\frac{1}{4\Omega\sqrt{x}}\Big(\exp\Big(-\frac{1}{2\Omega}\sqrt{x}\Big)\Big)^{m-1-k}$$
$$\Big(1-\exp\Big(-\frac{1}{2\Omega}\sqrt{\frac{x}{\gamma_{th}}-\frac{(1-\alpha)}{\xi\alpha}}\Big)\Big)^{N+k-i-m+1}dx+\frac{1}{(m-k-1)}\Bigg[\Big(\exp\Big(-\frac{1}{2\Omega}\sqrt{\frac{\gamma_{th}(1-\alpha)(1+\gamma_{th})}{\xi\alpha}}\Big)\Big)^{m-k-1}-$$
$$\Big(\exp\Big(-\frac{1}{2\Omega}\sqrt{\frac{\gamma_{th}(1-\alpha)}{\xi\alpha(1-\gamma_{th})}}\Big)\Big)^{m-k-1}\Bigg]\Big(1-\exp\Big(-\frac{1}{2\Omega}\sqrt{\frac{\gamma_{th}(1-\alpha)}{\xi\alpha}}\Big)\Big)^{N+k-i-m+1}\Bigg]. \tag{21}$$

$$R_2 = \sum_{k=0}^{m-2}\binom{m-2}{k}\frac{N!(-1)^{m-2-k}}{(N-m)!(m-2)!}\sum_{i=0}^{k}\binom{k}{i}\frac{(-1)^{k-i}}{k+N-i-m+1}\Bigg[\sum_{p=0}^{m-k-2}\binom{m-k-2}{p}\frac{(-1)^{m-k-p-2}}{N-i-p}\Big(1-\Big(1-$$
$$\exp\Big(-\frac{1}{2\Omega}\sqrt{\frac{\gamma_{th}(1-\alpha)}{\xi\alpha(1-\gamma_{th})}}\Big)\Big)^{N-i-p}\Big)-\frac{1}{(m-k-1)}\Big(\exp\Big(-\frac{1}{2\Omega}\sqrt{\frac{\gamma_{th}(1-\alpha)}{\xi\alpha(1-\gamma_{th})}}\Big)\Big)^{m-k-1}$$
$$\Big(1-\exp\Big(-\frac{1}{2\Omega}\sqrt{\frac{\gamma_{th}(1-\alpha)}{\xi\alpha}}\Big)\Big)^{N+k-i-m+1}\Bigg]. \tag{22}$$

$$I_2 = \sum_{k=0}^{m-2}\binom{m-2}{k}\frac{N!(-1)^{m-2-k}}{(N-m)!(m-2)!}\sum_{i=0}^{k}\binom{k}{i}\frac{(-1)^{k-i}}{k+N-i-m+1}\Bigg[\int_{x=\gamma_{th}(1+\gamma_{th})(1-\alpha)/\xi\alpha}^{\infty}\frac{1}{4\Omega\sqrt{x}}\Big(\exp\Big(-\frac{1}{2\Omega}\sqrt{x}\Big)\Big)^{m-1-k}$$
$$\Big(1-\exp\Big(-\frac{1}{2\Omega}\sqrt{\frac{x}{\gamma_{th}}-\frac{(1-\alpha)}{\xi\alpha}}\Big)\Big)^{N+k-i-m+1}dx-\frac{1}{(m-k-1)}\Big(\exp\Big(-\frac{1}{2\Omega}\sqrt{\frac{\gamma_{th}(1-\alpha)(1+\gamma_{th})}{\xi\alpha}}\Big)\Big)^{m-k-1}$$
$$\Big(1-\exp\Big(-\frac{1}{2\Omega}\sqrt{\frac{\gamma_{th}(1-\alpha)}{\xi\alpha}}\Big)\Big)^{N+k-i-m+1}\Bigg]. \tag{23}$$

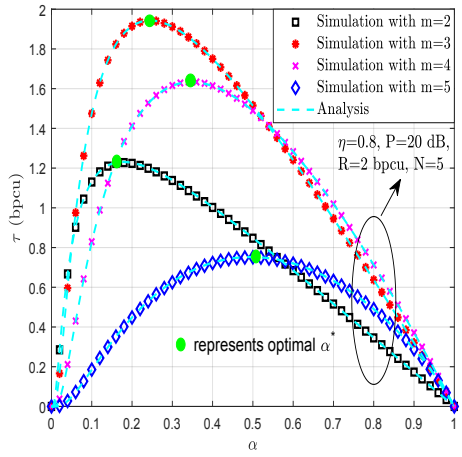

Fig. 7: τ *vs* α.

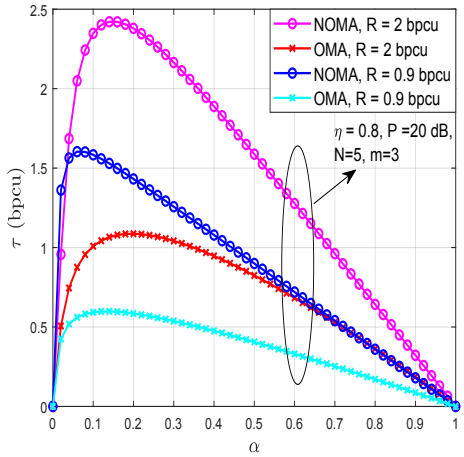

Fig. 8: τ *vs* α for different R.

better option at high target rates. In most IoT applications, the target rates are low, and energy considerations and the need to provide service to a large number of nodes become important. The analysis presented in this paper is clearly of great practical importance.

In Fig. 9, we plot throughput vs rate for different values of m (user $U_{(N)}$ and user $U_{(m)}$ selected together). Initially, throughput increases with an increase in rate, and then attains a maximum value at a certain rate value. A further increase in rate causes an increase in outage probability, which in turn results in a decrease in throughput. Therefore operating the system at the optimum target rate can result in maximum throughput.

VI. CONCLUSION

Due to the ever-increasing number of energy-constrained machine-type devices (MTDs), analyzing the performance of networks with energy-harvesting green self-sustaining MTDs is essential. In this article, we analyzed the performance of a NOMA-based uplink signalling with energy-harvesting IoT users assuming that the time-switching protocol is used for harvesting the energy. We allow concurrent transmission by two users in the uplink and derive expressions for the system throughput and outage probability. Out of N users, the optimum user selection mechanism selects the user with the best link SNR along the one having the m^{th} largest SNR, with the throughput optimal choice of m dependent on various

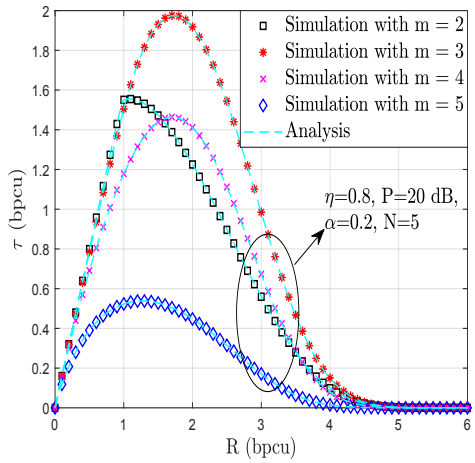

Fig. 9: τ *vs* R.

parameters. From the simulation results and the analysis, it is seen that an optimal value of the time-switching protocol exists for a particular user pair. In the extended version of this paper, different user selection schemes will be considered, and the analysis will be generalized to arbitrary number of users.

REFERENCES

[1] H. Zheng, S. Hou, H. Li, Z. Song, and Y. Hao, "Power allocation and user clustering for uplink MC-NOMA in D2D underlaid cellular networks," *IEEE Wireless Commun. Lett.*, vol. 7, no. 6, pp. 1030–1033, 2018.

[2] A. A. Nasir, X. Zhou, S. Durrani, and R. A. Kennedy, "Relaying protocols for wireless energy harvesting and information processing," *IEEE Trans. Wireless Commun.*, vol. 12, no. 7, pp. 3622–3636, 2013.

[3] H. Tabassum, M. S. Ali, E. Hossain, M. J. Hossain, and D. I. Kim, "Uplink vs. downlink NOMA in cellular networks: Challenges and research directions," in *2017 IEEE 85th Vehicular Technology Conference (VTC Spring)*, 2017, pp. 1–7.

[4] N. Jayanth, P. Chakraborty, M. Gupta, and S. Prakriya, "Performance of semi-grant free uplink with non-orthogonal multiple access," in *31st IEEE PIMRC*, 2020, pp. 1–6.

[5] S. Modem and S. Prakriya, "Optimization of links with a battery-assisted time-switching wireless energy harvesting relay," *IEEE Syst. J.*, vol. 12, no. 4, pp. 3044–3051, 2018.

[6] K. Agrawal, A. Jee, U. Makhanpuri, and S. Prakriya, "Performance of full-duplex cooperative NOMA with mode switching and an EH near user," *IEEE Networking Letters*, pp. 1–1, 2022.

[7] K. Agrawal, S. Prakriya, and M. F. Flanagan, "Optimization of SWIPT with battery-assisted energy harvesting full-duplex relays," *IEEE Trans. Green Commun. Netw.*, vol. 5, no. 1, pp. 243–260, 2021.

[8] P. D. Diamantoulakis, K. N. Pappi, Z. Ding, and G. K. Karagiannidis, "Wireless-powered communications with non-orthogonal multiple access," *IEEE Trans. Wireless Commun.*, vol. 15, no. 12, pp. 8422–8436, 2016.

[9] S. K. Zaidi, S. F. Hasan, and X. Gui, "Evaluating the ergodic rate in SWIPT-aided hybrid NOMA," *IEEE Commun Lett*, vol. 22, no. 9, pp. 1870–1873, 2018.

[10] T. A. Zewde and M. C. Gursoy, "NOMA-based energy-efficient wireless powered communications," *IEEE Trans. Green Commun. Netw.*, vol. 2, no. 3, pp. 679–692, 2018.

[11] Z. Ni, Z. Chen, Q. Zhang, and C. Zhou, "Analysis of RF energy harvesting in uplink-NOMA IoT-based network," in *2019 IEEE 90th Vehicular Technology Conference (VTC2019-Fall)*, 2019, pp. 1–5.

[12] A. Rauniyar, P. E. Engelstad, and O. N. Østerbø, "On the performance of bidirectional NOMA-SWIPT enabled IoT relay networks," *IEEE Sensors J.*, vol. 21, no. 2, pp. 2299–2315, 2021.

[13] M. Gupta and S. Prakriya, "Performance of CSI-based power control and NOMA/OMA switching for uplink underlay networks with imperfect SIC," *IEEE Trans. Cogn. Commun. Netw.*, vol. 8, no. 4, pp. 1753–1769, 2022.

[14] A. Bletsas, A. Khisti, D. Reed, and A. Lippman, "A simple cooperative diversity method based on network path selection," *IEEE J. Sel. Areas Commun.*, vol. 24, no. 3, pp. 659–672, 2006.

[15] H. A. David and N. Nagaraja, *Order Statistics*. 3rd ed. New York, NY, USA: Wiley, 2003.

[16] I. S. Gradshteyn and I. M. Ryzhik, *Table of Integrals, Series, and Products*. 7th ed. San Diego, CA, USA: Academic, 2007.